

## Dynamics of the far-infrared photoresponse in quantum Hall systems

N. G. Kalugin,<sup>1</sup> Yu. B. Vasilyev,<sup>2</sup> S. D. Suchalkin,<sup>2</sup> G. Nachtwei,<sup>1</sup> B. E. Sagol,<sup>1</sup> and K. Eberl<sup>3</sup>  
<sup>1</sup>*Institut für Technische Physik, TU-Braunschweig, Mendelssohnstrasse 2, D-38106 Braunschweig, Germany*  
<sup>2</sup>*A. F. Ioffe Physical Technical Institute, Polytekhnicheskaya 26, 194021 St.-Petersburg, Russia*  
<sup>3</sup>*Max-Planck-Institut für Festkörperforschung, Heisenbergstrasse 1, D-70569 Stuttgart, Germany*  
 (Received 19 April 2002; published 12 August 2002)

We have studied the time evolution of the far-infrared photoresponse of two-dimensional electron systems in the quantum Hall (QH) regime. We have identified different contributions to the photoresponse by using different sample geometries and by changing the direction of the magnetic field. In general, we have found a fast response (microseconds) related to photoinduced Hall currents, and longer response times (up to some hundreds of milliseconds) related to the photoinduced longitudinal resistance. Both types of the response are present in the bolometric response bound to the flanks of the QH plateau, and in the cyclotron resonance signal bound to the photon energy of the probe radiation. We give a qualitative explanation of our results on the basis of impurity-induced potentials for the localization of excited carriers.

DOI: 10.1103/PhysRevB.66.085308

PACS number(s): 73.43.-f, 78.47.+p, 73.50.Pz

### I. INTRODUCTION

Quantum Hall (QH) systems<sup>1</sup> develop typically Landau gaps of the order of 10 meV. Therefore, these systems can interact effectively with far-infrared (FIR) radiation with wavelengths of the order of 100  $\mu\text{m}$ . A considerable variety of results concerning the interaction of FIR radiation and QH systems has been published within the last 2 decades: starting from investigations applying molecular gas lasers<sup>2-5</sup> over measurements with Fourier-transform spectrometer<sup>6-12</sup> up to the application of tunable *p*-Germanium lasers.<sup>13-15</sup> Some studies in this field were focused on the interplay between QH edge states and FIR excitation.<sup>16-19</sup>

Despite a considerable amount of basic research on the interaction between FIR radiation and QH systems (for an overview, see Refs. 2-6, 12-14), the underlying mechanisms of the photoresponse (PR) are still a subject of controversy, and the dynamics of the photoexcited carriers in QH systems is still a subject of discussion.

Whereas earlier papers<sup>3-5</sup> show clearly both bolometric and resonant contributions to the FIR photoconductivity of QH samples, in recent papers<sup>6,9,12</sup> the response is completely attributed to bolometric contributions of the *longitudinal* resistivity. Whereas early papers<sup>3-5</sup> reported about *coexistence* of fast (about 10  $\mu\text{s}$ ) and slow (milliseconds) components of photosignals, in the recent papers<sup>10,12</sup> the entire photoresponse of a QH system was described via single exponentially decaying component with a parameter-dependent decay time, continuously tunable in region between a few microseconds and a few milliseconds.

The FIR investigations of QH systems are also interesting from the applicative point of view. The meander-shaped QH devices reach sensitivities as high as  $10^8$  V/W and a noise equivalent power of  $10^{-14}$  W/(Hz)<sup>1/2</sup> (Refs. 11 and 12). The high spectral selectivity (the width of excitation spectrum of about 2-5  $\text{cm}^{-1}$ —Refs. 7, 8, and 11), and the spectral tunability by changing the magnetic field, or by changing the concentration of the two-dimensional electron system

(2DES) of the QH detector, is a unique property in comparison with other FIR detectors.

In our study, we have investigated QH systems of different shapes (Hall bars, meander-shaped devices) under various conditions in order to obtain detailed information on the limits of the detector performance and on the underlying mechanisms. Using the radiation of a pulsed tunable *p*-Ge FIR laser, we have distinguished clearly bolometric and cyclotron-resonant, and also longitudinal and *transversal* (due to photoinduced Hall currents) signal contributions. We observe fast (few microseconds) and slow *coexisting* response times, and attribute the fastest part of the PR to the transversal components.

### II. SAMPLE DETAILS AND EXPERIMENTAL TECHNIQUE

Our samples are two GaAs/AlGaAs heterostructures (wafer A and wafer B) with the following parameters: wafer A has the two-dimensional electron density  $n_s = 3.11 \times 10^{11} \text{ cm}^{-2}$  and the mobility  $\mu_{4.2\text{K}} = 190\,000 \text{ cm}^2/\text{V s}$ , for wafer B the corresponding parameters are  $n_s = 2 \times 10^{11} \text{ cm}^{-2}$ ,  $\mu_{4.2\text{K}} = 500\,000 \text{ cm}^2/\text{V s}$ . These wafers were patterned in different geometries (270- $\mu\text{m}$ -wide, 2-mm-long Hall bars; and 100- $\mu\text{m}$ -wide, 60-mm-long, meander-shaped samples,  $2 \times 3 \text{ mm}^2$  square). The probe emission source in our experiment was a *p*-Ge pulsed cyclotron laser (pulse width about 1  $\mu\text{s}$ , repetition rate 1 Hz, maximal peak power about 1 W, linewidth of the radiation about  $0.2 \text{ cm}^{-1}$ ) which is tunable around a wavelength of 100  $\mu\text{m}$  by an external magnetic field (for a description of the functional principle, see Ref. 20). This allows us to make the time resolved measurements around filling factor  $\nu = 2$  for a wide range of electron concentrations of 2DES in the QH samples. The photoresponse (photoinduced change of longitudinal voltage,  $\Delta V_x$ ) of the samples was measured via a single high-frequency cable (maximum frequency 36 GHz, 50 $\Omega$ ). The corresponding time constant (sample resistance multiplied by cable capacitance) was of the order of 1  $\mu\text{s}$  and thus comparable with the response time of the fast parts of the observed

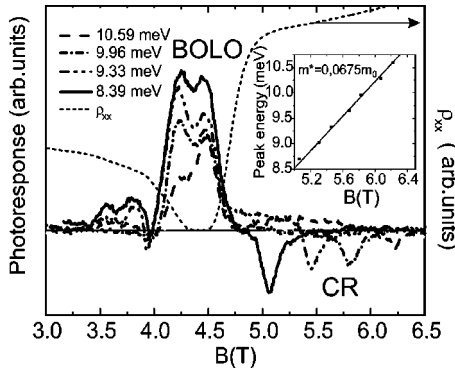


FIG. 1. The time-integrated magnetic field dependence of the photoresponse of a Hall bar sample (wafer B) at different photon energies of a *p*-Ge laser radiation, maximal laser intensity  $J_{\max}$  (corresponds to peak power about 1 W), bias current 45  $\mu\text{A}$ ,  $T=4\text{ K}$ . The inset demonstrates the linear dependence of the cyclotron resonance (CR) line on the magnetic field.

signal. The sample current was varied typically from  $0.1I_c$  to up to  $3I_c$  ( $I_c$  is the critical current of the QHE breakdown).

### III. EXPERIMENTAL RESULTS

In Fig. 1, the photoresponse (PR) of a Hall bar (wafer B) is shown as a function of the magnetic field for different positions of the laser line. Whereas the double peak inside the plateau remains bound to the flanks of the QH plateau (bolometric response), the negative peak moves with the laser line, yielding a cyclotron mass of  $m_c=0.067m_0$ , where  $m_0$  is the free electron mass (cyclotron resonance, CR). An important result is that the signal of the photoresponse in Hall bars is fast (signals with a rise time of the order of the rise time of the FIR pulse, and decay times of about 1–6  $\mu\text{s}$  depending on the nature of the response), and the initial part of the signal changes the sign with the change of the direction of the magnetic field of the sample (Fig. 2). This means that the signal of PR in the first microseconds after the pulse of FIR radiation is mainly the result of the drift component of photoexcited electrons in the direction of the Hall field. The initial period of time evolution of the relaxation of the photoexcited electrons is significantly defined by the current flowing *across* the sample, causing the fast part of longitudinal PR in QH systems. Thus, we can write the expression for the longitudinal photoresponse  $\Delta V_x$  of QH system as follows:

$$\Delta V_x = (\Delta\rho_{xx}^{\text{bolom}} + \Delta\rho_{xx}^{\text{CR}})(L/w)I_{\text{bias}} + (\rho_{xy} + \Delta\rho_{xy}^{\text{bolom}} + \Delta\rho_{xy}^{\text{CR}})I_H^{\text{photo}}, \quad (1)$$

where  $\Delta\rho_{ij}^{\text{bolom}}$  is the bolometric part of the photoinduced change of  $\rho_{ij}$ , which is proportional to  $\partial\rho_{ij}/\partial T_e$  ( $T_e$  is the electron temperature);  $\Delta\rho_{ij}^{\text{CR}}$  is the CR-related photoinduced change of  $\rho_{ij}$ ,  $I_{\text{bias}}$  is the source-drain (bias) current;  $I_H^{\text{photo}}$  is the photoinduced current along the Hall field, changing the sign with the change of the direction of the magnetic field;  $L$  is the length; and  $w$  is the width of the QH sample.

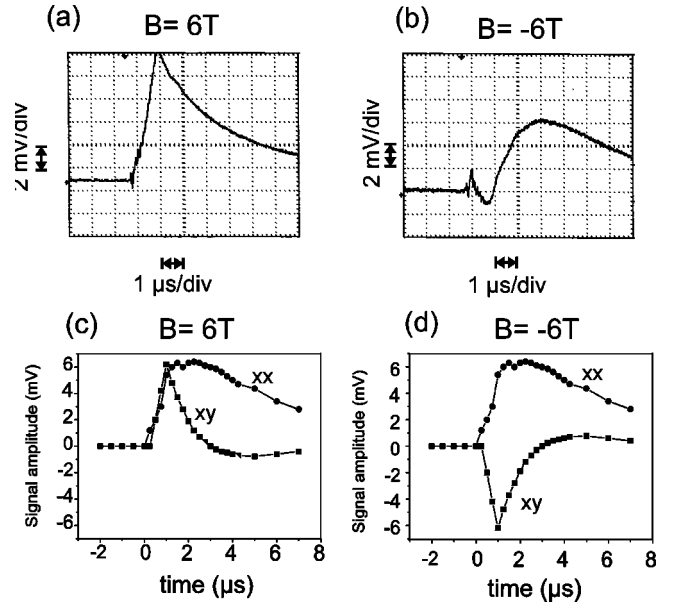


FIG. 2. The time evolution of PR of the Hall bar sample (wafer A) at  $B = \pm 6\text{ T}$  for two opposite field directions [(a) and (b)],  $T = 4\text{ K}$ , bias current 50  $\mu\text{A}$ , photon energy of a laser radiation 9.8 meV,  $J_{\max}$ , direct signal from the sample (no amplifiers). The dependencies show the presence of both the Hall-field-related part of PR (during initial 2–3  $\mu\text{s}$  of a signal evolution), and of the longitudinal component (with a decay time  $\tau$  of about 4–6  $\mu\text{s}$ ) which does not change the polarity with the change of the magnetic field orientation. (c) and (d) The results of numerical separation of this transversal (marked by *xy*) and longitudinal (*xx*) components from the data of (a) and (b). (c) The *xx* and *xy* components, the sum of which gives (a); (d) shows how the same *xx* component, and the *xy* component after the sign inversion (due to change of the magnetic field direction into opposite,  $B+ \rightarrow B-$ ), in sum are giving (b).

In contrast, just the first term of Eq. (1) was mentioned in many previous works.<sup>7–13</sup> Consequently for the bolometric photoresponse, we should take into account not only the temperature derivative of the longitudinal resistance, but also the contributions of the transversal resistance [see Eq. (1)]. This explains the details of the spectral shape of the photoresponse in Fig. 1, such that the low field part of the photoresponse curve (the part of negative polarity at about 4 T), near the QH plateau, is the part of bolometric signal caused by  $\partial\rho_{xy}/\partial T_e$  [see Fig. 3(b)]. Equation (1) shows that the resulting polarity of PR for both the bolometric and the nonbolometric CR-related part, in reality can be of any sign, either negative or positive. The signal polarity depends on the mutual orientation of the bias current and the Hall field in the sample, and on the weights of different components of the signal. These weights of the components, in their own order, depend on the magnetic field, on the value of the bias current, on the intensity and on the wavelength of the applied FIR radiation.

A similar field dependence of the polarity of PR was observed in Ref. 3 for the microwave photoresponse of QH systems, which can also be described by expression (1).

In addition to the fast immediate few-microsecond-long photoresponse, slow components of PR appears a few milli-

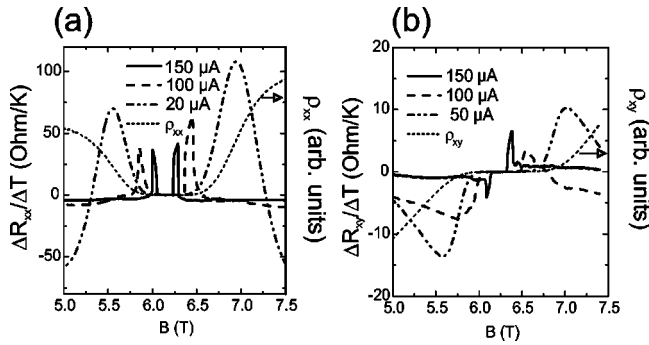


FIG. 3. (a) The experimentally measured ratio  $\Delta R_{xx}/\Delta T$ , where  $\Delta R_{xx}$  is the deviation of the longitudinal resistance of a sample, caused by  $\Delta T$ , which is the change of the sample temperature from 1.6 to 4 K, for the Hall bar sample (wafer A), at different bias currents (see the legend). The  $\rho_{xx}(B)$  curve at bias current  $5 \mu\text{A}$ ,  $T=4 \text{ K}$ , is shown as the guideline. (b) The ratio  $\Delta R_{xy}/\Delta T$ , measured in the same experiment with (a). The  $\rho_{xy}(B)$  curve at  $5 \mu\text{A}$ ,  $4 \text{ K}$ , is shown as the guideline.

seconds after the FIR pulse. In Hall bars these components are relatively weak. These components appear in the signal, if the magnetic field of a sample is at the edges of the QH plateau, or lies outside of the plateau. Thus, we observe the long decay times in the PR, as previously reported in Refs. 3 and 5. Also, we can confirm the weak dependence of the bolometric part on the wavelength of the FIR radiation (see Fig. 1), as reported in Ref. 3.

When we investigate samples with meander geometry in comparison with Hall bars (with a length of the meander sample, which is by orders of magnitude bigger than the width), the role of longitudinal,  $\rho_{xx}$ -related components of PR is dramatically increased. The PR remains spectrally similar (Fig. 4), but changes its temporal behavior. Rather long response times (with decay times of about  $300\text{--}350 \mu\text{s}$ ) appear in the PR signals (Fig. 5), and these long time components do not change the sign with the orientation of the magnetic field of sample. At the same time the fast (about  $6\text{--}8 \mu\text{s}$  decay time in all meander samples under study), field direction-dependent part of PR, also occurs in meanders as in the Hall bar samples, and moreover grows in amplitude with the increase of the length of the sample. This is understandable: the Hall current appears after the FIR pulse in the cross sections of the sample in regions with a local increase of the Hall field (due to potential fluctuations), and the increase of the length of the sample increases the number of such regions. The current occurs due to the appearance of hot photoexcited electrons or/and due to QH breakdown if the bolometric part of PR near the QH plateaus is considered. The photoresponse, being as long as a millisecond, tens and even hundreds of milliseconds, also remains in the meander samples. This long-time part of PR is much more stable and pronounced in meanders than in Hall bars (Fig. 5).

The results on the meanders nicely illustrate the details of the bolometric part of the PR. Figure 6 demonstrates the field dependencies of PR for the bolometric PR near the filling factor  $\nu=2$  for the PR magnitude measured with different time delays after the FIR pulse. It is clearly seen that the Hall

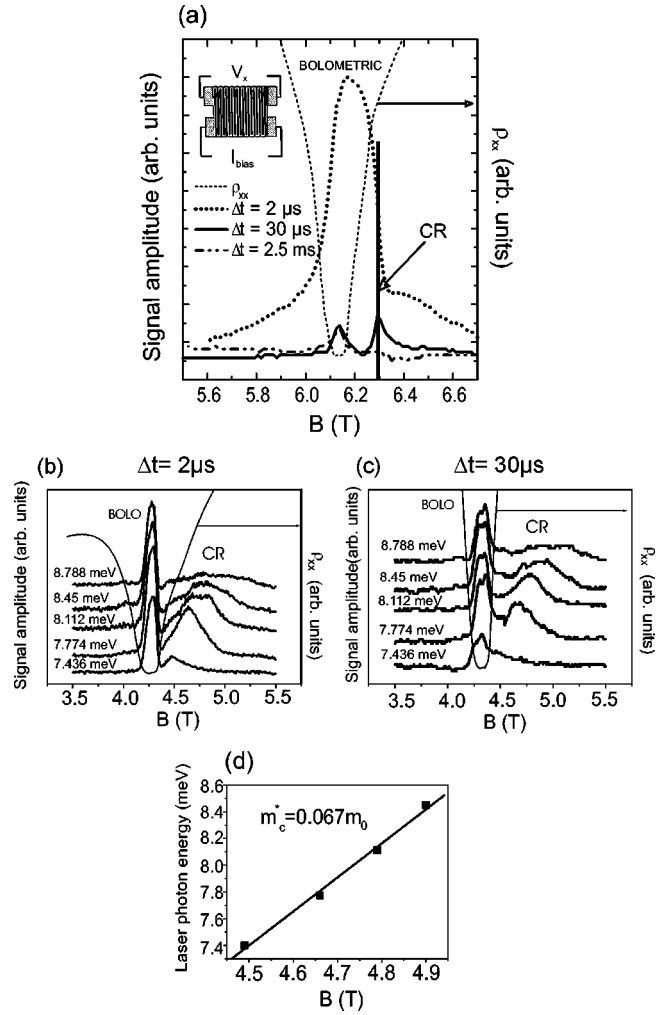


FIG. 4. (a) The magnetic field dependence of the PR at different stages of the signal evolution. Here  $\Delta t$  is the time delay after the start of  $p\text{-Ge}$  lasing. The meander-shaped sample (wafer A),  $T = 4 \text{ K}$ , bias current  $I_{\text{bias}} = 60 \mu\text{A}$ , laser photon energy  $10.78 \text{ meV}$ , maximal intensity of radiation. (The inset shows the scheme of design of the meander QH samples). The bolometric and CR parts of PR (indicated) overlap at the early times of relaxation, but are clearly distinguishable after a few tens of microseconds. The  $\rho_{xx}(B)$  curve is shown as the guideline. (b), (c) The magnetic field dependence of PR of the meander sample (wafer B) at different laser photon energies,  $J_{\text{max}}$ , bias current  $25 \mu\text{A}$ ,  $T=4 \text{ K}$ . Here (b) corresponds to the early stage of PR with the delay time  $\Delta t = 2 \mu\text{s}$ , consisting mainly of Hall part of PR with the decay time  $\tau = 6\text{--}8 \mu\text{s}$ , (c) corresponds to  $\Delta t = 30 \mu\text{s}$  and represents mainly the longitudinal component with  $\tau = 350 \mu\text{s}$ . The scale of vertical axis on (c) is 5 times smaller than that for (b); the  $\rho_{xx}(B)$  curve is shown in (b) and (c) as the guideline; (b) and (c) clearly demonstrate the dynamics of relaxation on the example of the bolometric PR: shortly after the FIR pulse, the QH plateau shrinks [we observe a single peak—see (b)], after  $30 \mu\text{s}$  we already observe the double-peak structure [see (c)], i.e., the QH plateau returning back to the initial width as it was before the FIR pulse. (d) The dependence of the CR line energy on the magnetic field, from the data of (b) and (c).

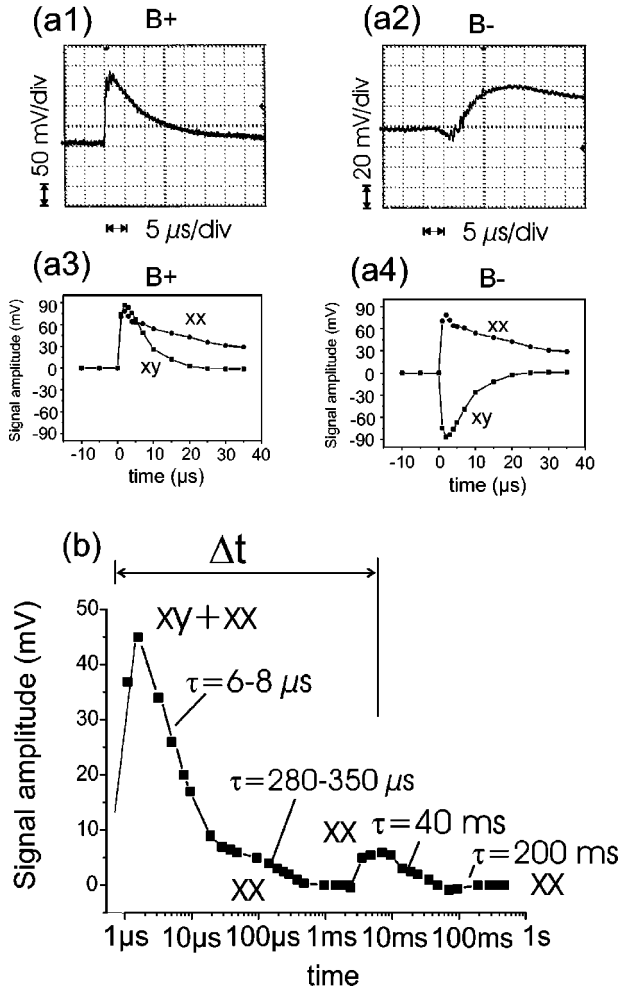


FIG. 5. (a1)–(a4). The time dependence of the bolometric part of PR of the meander-shaped sample (wafer A).  $T = 4$  K,  $J_{\max}$ . Here (a1), (a2) show the early stage of PR at two opposite directions of the magnetic field for  $B = \pm 5.9$  T,  $I_{\text{bias}} = 25 \mu\text{A}$ , laser photon energy 10.92 meV, signal was recorded directly from the sample (no amplifiers); (a3), (a4) represent the results of numerical separation of the Hall ( $xy$ ) and longitudinal ( $xx$ ) components of PR from the traces in (a1) and (a2). (b) The entire time dependence of PR on the example of PR trace of the meander sample (wafer B), laser photon energy 7.774 meV,  $J_{\max}$ , bias current  $50 \mu\text{A}$ ,  $T = 4$  K. One can clearly see the earlier mentioned parts of PR with different  $\tau$ , and the meaning of  $\Delta t$ . We have selected  $\Delta t = 2 \mu\text{s}$  and  $\Delta t = 30 \mu\text{s}$  in our scans vs magnetic field, because in the first case it gives the information about fast Hall  $xy$  component of the PR; and after  $30 \mu\text{s}$  the PR is almost completely defined only by longitudinal ( $xx$ ) part of PR.

current-related fast component of PR is larger than the longitudinal components even in the meander samples, if we consider the bolometric PR.

The double peak structure, following  $\partial \rho_{ij} / \partial T_e$ , has a closer distance between the peaks for the fast component, and then the distance between the peaks grows with time. Thus, we really see the electronic bolometricity, because on the microsecond scale the distribution of electrons obviously already can be described by the electron temperature  $T_e$ , which slowly (in milliseconds) decreases and finally reaches

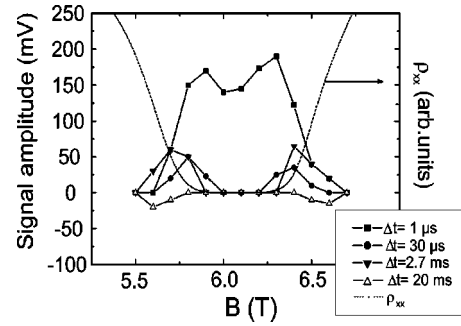


FIG. 6. The picture of relaxation of the magnetic field dependence of a bolometric PR in the meander-shaped sample (wafer A),  $I_{\text{bias}} = 25 \mu\text{A}$ , laser line at 10.91 meV, maximal laser intensity. The field dependence at  $\Delta t = 1 \mu\text{s}$  [mainly defined by fast (field-direction dependent) component with a decay time  $\tau = 6-8 \mu\text{s}$ ], for the part of PR which appears almost simultaneously with a FIR pulse, is a product of the superposition of two peaks, bound to the flanks of the QH plateau. With time (see the field dependencies for longitudinal PR components with  $\Delta t = 30 \mu\text{s}$  (when it is mainly the part of longitudinal PR with  $\tau = 350 \mu\text{s}$ ,  $\Delta t = 2.7$  ms and  $\Delta t = 20$  ms), the distance between these two peaks grows. They return back to the positions of the QH plateau flanks before the FIR pulse, as defined by the bias current.

the temperature of the lattice. The FIR pulse excites hot electrons and destroys the equilibrium distribution of the carriers. The system quickly reacts with a fast (it takes not longer than  $1 \mu\text{s}$ ) shrinking of the QH plateau. The FIR pulse causes the appearance of a Hall current. Then the system relaxes back to the initial width of the plateau. This behavior is also seen in Figs. 4(b) and 4(c), where after  $\Delta t = 2 \mu\text{s}$  we see effectively a single peak of bolometric PR, and after  $30 \mu\text{s}$  a double-peak dependence develops.

It is known<sup>21</sup> that the bias current itself leads to the creation of hot electrons and to the breakdown of the QH effect. FIR radiation is just another mechanism to generate hot non-equilibrium electrons. In that sense the effects of bias current and FIR radiation are somehow competing: having a lower current and a higher intensity of excitation, or a higher current and a lower FIR intensity, we can reach quite similar physical situations. For example, at high FIR excitation we can easily observe the merge of two peaks of the bolometric PR to an effectively single-peak field dependence (as it was described in Ref. 14), and the same effect can be observed just by increasing the bias current.

The bolometric and resonant components of the PR demonstrate the difference not only in the magnetic field dependences. They are also different in dependence on the bias current. For the bolometric part of PR, the bias current dependence for the fast Hall field-related part of PR is almost linear (see Fig. 7) independently of the position of laser line. This simply reflects the linear dependence of the Hall field, and therefore of the photoinduced Hall current in the QH system, on the bias current. At the same time, the CR-related part of PR has another bias current dependence. Despite the fact that the fast part of PR is (as in the case of bolometric PR) clearly Hall-field dependent, and changes the sign with the change of the direction of the sample magnetic field (see

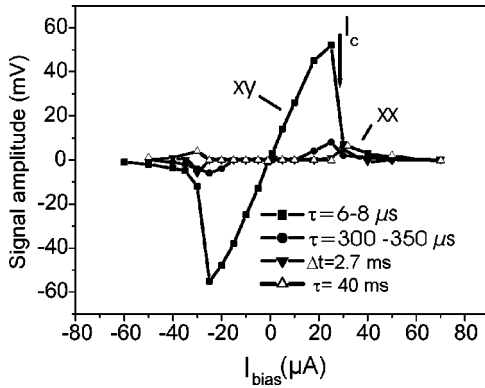


FIG. 7. The dependence on the bias current for different components of the bolometric PR.  $T=4$  K, meander sample (wafer B),  $B=4.28$  T, laser position 7.774 meV (CR at 4.5 T),  $J_{\max}$ . The arrow demonstrates the position of  $I_c$ .

Fig. 8), in the case of CR response the bias current dependence is clearly nonlinear. The interesting aspect is that the nonlinearity for the CR PR-dependence appears at the bias currents, where the current-voltage characteristic of the sample is still linear (at the measurement position the longitudinal voltage on the sample grows linearly with the bias current until about  $20\mu\text{A}$ ).

In our experiments, for the Hall bars the time dependencies of the PR for the bolometric signal and the CR resonance were similar at all applied radiation intensities. In Hall bars, we did not find any observable dependence of the time constants on the mobility of samples.<sup>15</sup> In meanders in our experiments (with the laser intensities we used) the time constants of PR also demonstrate no dependence on the sample mobility, in contrast to data of Refs. 10 and 12. For all samples under study we observed a fast Hall component (of

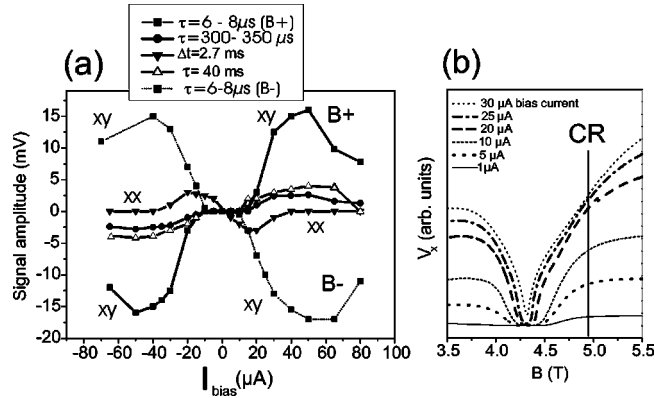


FIG. 8. (a) The dependence on the bias current for different components of the cyclotron resonance PR, for the meander (wafer B),  $J_{\max}$ ,  $T=4$  K. The results in (a) were obtained under  $B = \pm 4.875$  T, laser at 8.45 meV (cyclotron resonance). The change of magnetic field direction changes the polarity of the fast ( $\tau=6-8\mu\text{s}$ ) transversal (Hall) component of PR [see (a), cases  $B+$  and  $B-$ ]. The measurement position (precise CR) is shown in (b). (b) The magnetic field dependence of the longitudinal voltage  $V_x$  for the same sample at different bias currents, no FIR illumination.

about 6- to  $8\text{-}\mu\text{s}$  decay time), a slow component (of about 300- to  $350\text{-}\mu\text{s}$  decay time), and a slow millisecond-component if we were out of the QH plateau. In the samples with low mobility, the sensitivity at the CR is low, and the CR line is observable only at relatively high bias currents even at the highest applied intensities of laser radiation. With increasing sample mobility the CR-related sensitivity grows. Although it is usually argued that the semi-insulating substrate should not affect the PR, a possible influence of substrate heating by the intense laser pulses due to resonant interaction with impurities cannot be completely excluded. However, no distinct lines, which could be attributed to this effect, could be detected.

#### IV. DISCUSSION

To summarize our experimental results, for the FIR photoreponse in QH systems we have observed: (1) the major importance of the Hall field, (2) the existence of a dependence of the sensitivity of QH systems on the mobility for the CR-related part of the PR, which indicates the importance of random potential and localization of carriers in this potential; (3) the observed difference of the PR decay times for  $xx$  and  $xy$  components.

These facts lead us to the conclusion that in QH systems a Hall field-induced anisotropy of scattering and localization may occur. The random potential-related localization regions (Fig. 9) are not isotropic in the presence of the Hall field. Because of this Hall field, the localization “lakes” should be larger in size in the direction along the Hall field. During the FIR pulse, we create excited electrons, which move easier along the Hall field: with less scattering events (on the random potential) than in the perpendicular (to the Hall field) direction. Moreover, in the initial time after the pulse we should have the appearance of an effective “flattening”—a reduction of the importance of the random potential along the Hall field due to screening, i.e., the “lakes” should transform into stripes. Then, the relaxation of system means the relaxation from such a strongly anisotropic stripe-like localization potential back to more isotropic case. Naturally, for the CR-related effects (which are bound to the degree of scattering and thus to the disturbance of the free motion of electrons along the cyclotron orbit) the changes in size, dimensions, and shape of the regions in which the electrons can move, should affect the CR-part of the PR. Consequently, the higher mobility samples, having larger fluctuation length scales and better conditions for CR, can show a more pronounced sensitivity of the CR.

On the basis of our results, we would like to comment on some conclusions made in some previous works on the mechanisms of the FIR photoreponse of the QH systems (Refs. 6, 9, 11, and 12). Many previous conclusions were based on the results of experiments where the authors used the nonmonochromatic wide-range FIR radiation, and long durations of pulses. Under such conditions it was technically impossible to distinguish different components of PR. For example, the conclusion that the entire FIR longitudinal photoreponse of QH system is proportional to  $(\partial\rho_{xx}/\partial T)\Delta T_e$  and can be completely explained via this single term was

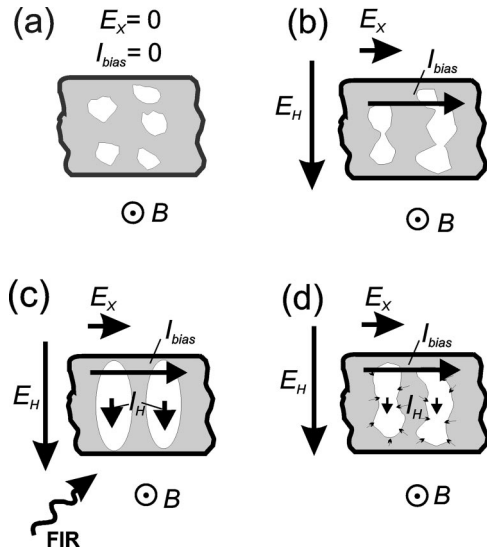


FIG. 9. The possible evolution of an electron localization picture in our experiment. (a) The picture of a localization potential in a part of a QH sample before application of the source-drain field and appearance of the bias current  $I_{\text{bias}}$ . (b) The picture of the localization potential before the FIR pulse. The regions of localization are larger in size along the Hall field  $E_H$  ( $E_H$  is about  $10E_x$  (after the QH breakdown), where  $E_x$  is the longitudinal component of the electric field inside the QH sample). (c) The FIR pulse heats the electron system and causes the transitions of electrons to higher Landau levels. The sample reacts by the transformation of the localization regions into “stripes,” and by the appearance of the Hall current  $I_H^{\text{photo}}$  [the profile of the scattering potential across the sample (screened potential fluctuations) differs from the profile along the sample (well developed fluctuations)]. (d) The picture some time after a FIR pulse.  $I_H^{\text{photo}}$  decreases and the regions of effective localization relax. The drift of “colder” electrons in the longitudinal field  $E_x$  and (in the case of CR) the processes of orbital and percolative motion of electrons in the relaxing regions become dominant.

initially based on the topological similarity of experimentally observed plateau-bound double-peak magnetic field dependencies of PR of QH systems, with the double-peak shape of the temperature derivative of  $\rho_{xx}$ . But, our results [see Fig. 4(b)] clearly demonstrate that the efficiency of nonbolometric CR-related part of PR is maximal at some intermediate distances from the flanks of QH plateau, and going down if we either increase the distance between position of CR and flanks of QH plateau, or if we go with CR position inside the QH plateau (in fact, inside the plateau the efficiency of CR is zero, as shown already in Ref. 3). That means that if we plot the dependence of CR efficiency of a QH system versus a magnetic field, we obtain just a wider, but looking similar to the bolometric one, double-peak structure around the QH plateau. So, if using the wide range polychromatic FIR radiation, for each magnetic field our QH system will receive the corresponding spectral part of radiation resonantly, and the rest via the bolometric mechanism. As a result we should indeed obtain the double-peak magnetic field dependence, which in reality will be the product of overlap of bolometric and CR efficiency curves.

The understanding of this fact allows us to explain the differences in the bias current dependence of PR for different magnetic field positions, observed in Ref. 11. The observed linear or nonlinear dependencies simply reflect the actual weights of bolometric, or of CR-related, mechanisms of PR for the given sample at the given magnetic field.

These arguments, the above-mentioned observation of the independence of the bolometric part on the laser line position, and previous results of spectroscopic investigations of QH detectors (see Refs. 7, 8, and 12: the spectrum of sensitivity of the QH detector demonstrated just the cyclotron resonance line even in the case of low FIR intensities) show that the PR of QH detectors cannot be interpreted as completely bolometric even at lowest FIR intensities.

Another possible complication in the recovery of the  $xy$  component of the PR can be due to the selected patterning geometry of our QH samples. Due to our experience, the decrease of the width of meander samples leads to an increase of the weight of the  $xx$  parts of PR. Therefore, the  $xy$  component of the PR was very effectively masked by the larger  $xx$  components.

In our results we confirm the coexistence of different time scales of the PR. Therefore, the description of the relaxation of photoexcited electrons via one monoexponential single decay time dependence (as in Refs. 10 and 12) appears to be questionable.

## V. SUMMARY

In conclusion, we have observed the existence of two components of the FIR photoresponse of quantum Hall systems—a transversal and a longitudinal component, each of it corresponding to two mechanisms of the photoresponse—the bolometric PR and the cyclotron-resonant PR. The transversal components of the PR decays within a few microseconds, the longitudinal components demonstrate longer decay times (a few microseconds to a few hundred microseconds), depending on the length of samples. Our results show that, using appropriate components of PR of QH system, we can produce FIR selective tunable detectors, which are not only 3 orders more sensitive (Ref. 12), but also 3 orders faster, than the conventional Si bolometers, working at the same temperature.

## ACKNOWLEDGMENTS

We thank Professor K.v. Klitzing, Professor R. J. Haug, Professor R. R. Gerhardt, and Dr. U. Zeitler for fruitful discussions, Professor I.V. Kukushkin for his contribution in the development of our experimental setup, and Dr. G. Hein for the preparation of meander samples. The work was supported by the Schwerpunktprogramm “Quanten-Hall-Systeme” of the Deutsche Forschungsgemeinschaft (DFG), Project No. Na235/10-1. Yu.V. and S.S. also acknowledge the Russian Fund for Basic Research and the Russian Program “Physics of Solid State Nanostructures” for partial support.

- <sup>1</sup>K. von Klitzing, G. Dorda, and M. Pepper, *Phys. Rev. Lett.* **45**, 494 (1980).
- <sup>2</sup>J. C. Maan, Th. Englert, D. C. Tsui, and A. C. Gossard, *Appl. Phys. Lett.* **40**, 609 (1982).
- <sup>3</sup>D. Stein, G. Ebert, K. von Klitzing, and G. Weimann, *Surf. Sci.* **142**, 406 (1984); D. Stein, Diplomarbeit, TU-München, 1983.
- <sup>4</sup>R. E. Horstmann, E. J. v. d. Broek, J. Wolter, R. W. v. d. Heijden, G. L. J. A. Rikken, H. Sigg, P. M. Frijlink, J. Maluenda, and J. Hallais, *Solid State Commun.* **50**, 753 (1984).
- <sup>5</sup>M. J. Chou, D. C. Tsui, and A. Y. Cho, *Proceedings of the 18th International Conference on Physics of Semiconductors* (World Scientific, Stockholm, 1986), p. 437.
- <sup>6</sup>K. Hirakawa, M. Endo, K. Yamanaka, Y. Hisanaga, and S. Komiyama, *Proceedings of the 23rd International Conference on Physics of Semiconductors* (World Scientific, Berlin, 1996), p. 2543.
- <sup>7</sup>V. I. Gavrilenko, I. V. Erofeeva, N. G. Kalugin, A. L. Korotkov, M. D. Moldavskaya, Y. Kawano, and S. Komiyama, *Proceedings of the Sixth International Symposium Nanostructures: Physics and Technology*, St. Petersburg, 1998, p. 497.
- <sup>8</sup>A. V. Antonov, I. V. Erofeeva, V. I. Gavrilenko, N. G. Kalugin, A. L. Korotkov, A. V. Maslovskii, M. D. Moldavskaya, S. I. Pripolzin, V. L. Vaks, Y. Kawano, and S. Komiyama, *Mater. Sci. Forum* **297–298**, 353 (1999).
- <sup>9</sup>K. Hirakawa, K. Yamanaka, Y. Kawaguchi, M. Endo, M. Saeki, and S. Komiyama, *Phys. Rev. B* **63**, 085320 (2001).
- <sup>10</sup>V. I. Gavrilenko, I. V. Erofeeva, O. Astaf'ev, I. Kawano, and S. Komiyama, *Proceedings of the Workshop "Nanophotonics," Nizhny Novgorod*, 2001, p. 196.
- <sup>11</sup>Y. Kawaguchi, K. Hirakawa, M. Saeki, K. Yamanaka, and S. Komiyama, *Appl. Phys. Lett.* **80**, 136 (2002).
- <sup>12</sup>Y. Kawano, Y. Hisanaga, H. Takenouchi, and S. Komiyama, *J. Appl. Phys.* **89**, 4037 (2001).
- <sup>13</sup>K. Unterrainer, C. Kremser, E. Gornik, and Yu. L. Ivanov, *Solid-State Electron.* **32**, 1527 (1989).
- <sup>14</sup>Yu. B. Vasilyev, S. D. Suchalkin, Yu. L. Ivanov, S. V. Ivanov, P. S. Kop'ev, and I. G. Savel'ev, *JETP Lett.* **56**, 377 (1992); S. Suchalkin, Yu. Vasilyev, Yu. Ivanov, S. Ivanov, P. Kop'ev, and T. Ohyama, *Solid-State Electron.* **40**, 469 (1996).
- <sup>15</sup>N. G. Kalugin, Yu. B. Vasilyev, S. D. Suchalkin, G. Nachtwei, B. E. Sagol, and K. Eberl, *Physica B* **314**, 166 (2002); *Physica E (Amsterdam)* **12**, 144 (2002).
- <sup>16</sup>R. Merz, F. Keilmann, R. J. Haug, and K. Ploog, *Phys. Rev. Lett.* **70**, 651 (1993).
- <sup>17</sup>R. J. F. van Haren, F. A. P. Blom, and J. H. Wolter, *Phys. Rev. Lett.* **74**, 1198 (1994).
- <sup>18</sup>A. Lorke, J. P. Kotthaus, J. H. English, and A. C. Gossard, *Phys. Rev. B* **53**, 1054 (1996).
- <sup>19</sup>B. G. L. Jager, S. Wimmer, A. Lorke, J. P. Kotthaus, W. Wegscheider, and M. Bichler, *Phys. Rev. B* **63**, 045315 (2001).
- <sup>20</sup>Yu. L. Ivanov and Yu. B. Vasilyev, *Sov. Tech. Phys. Lett.* **9**, 264 (1983); E. Gornik, K. Unterrainer, and C. Kremser, *Opt. Quantum Electron.* **23**, S267 (1991).
- <sup>21</sup>G. Ebert, K. v. Klitzing, K. Ploog, and G. Weimann, *J. Phys. C* **16**, 5441 (1983); G. Nachtwei, *Physica E (Amsterdam)* **4**, 79 (1999).